

# Current-induced microwave excitation of a domain wall confined in a magnetic wire with bi-axial anisotropy

Katsuyoshi Matsushita, Jun Sato, and Hiroshi Imamura

*Nanotechnology Research Institute (NRI),*

*Advanced Industrial Science and Technology (AIST),*

*AIST Tsukuba Central 2, Tsukuba, Ibaraki 305-8568, Japan.*

## Abstract

We studied the current-induced magnetization dynamics of a domain wall confined in a magnetic wire with bi-axial anisotropy. We showed that above the threshold current density, breathing-mode excitation, where the thickness of the domain wall oscillates, is induced by spin-transfer torque. We found that the breathing-mode can be applied as a source of microwave oscillation because the resistance of the domain wall is a function of the domain wall thickness. In a current sweep simulation, the frequency of the breathing-mode exhibits hysteresis because of the confinement.

Recent advances in spin electronics have revealed that the current flowing through a magnetic nanostructure with a non-collinear magnetization configuration can excite magnetization dynamics. Current-induced microwave generation has attracted a lot of attention because it will be a candidate for applications in future wireless telecommunication technologies. Most studies of current-induced microwave generation have been carried out in magnetic multilayers<sup>1,2,3,4,5,6,7,8</sup>. In these experiments, uniform precession of the free layer magnetization<sup>9,10</sup> is driven by spin-transfer torque<sup>11,12,13</sup>, and the motion of the free layer magnetization is measured using the CPP-GMR or TMR effect.

Only a few works have theoretically suggested on the current-induced microwave generation of a domain wall<sup>14,15</sup>. He and Zhang proposed an application of the oscillating motion of the domain wall under current and magnetic field as a source of microwave oscillation<sup>14</sup>. Ono and Nakatani proposed a microwave oscillator using the rotating motion of the domain wall<sup>15</sup>.

On the other hand, it is known that a domain wall produces an additional resistance in magnetic wires. According to the theory of Levy and Zhang<sup>16</sup>, the resistivity of a domain wall is inversely proportional to the square of the domain wall thickness. Therefore, if we excite a breathing-mode where the thickness of the domain wall oscillates by application of a dc current, we can use the oscillation as a microwave source. From the view point of physics, it is also important to study the current-induced magnetization dynamics (CIMD) of the geometrically confined domain wall since CIMD is in general different from magnetic-field-induced magnetization dynamics and little is known about the CIMD of a geometrically confined domain wall.

In this paper, we investigated the CIMD of a domain wall confined in a magnetic wire with bi-axial anisotropy by a confining potential due to the wire shape shown in Fig. 1(a). We showed for a confined domain wall that above the threshold current density, spin-transfer torque induces breathing-mode excitation<sup>17,18</sup>, where the thickness of the domain wall oscillates. The current-induced breathing-mode can be applied for a microwave oscillation because the resistance of the domain wall is a function of the domain wall thickness. We also found that if the current density is adiabatically changed, the frequency of the breathing-mode shows a hysteresis loop because the confining potential enables the breathing and pinning states to coexist below the threshold current density.

The system we consider is a 180° domain wall confined by a potential due to the wire

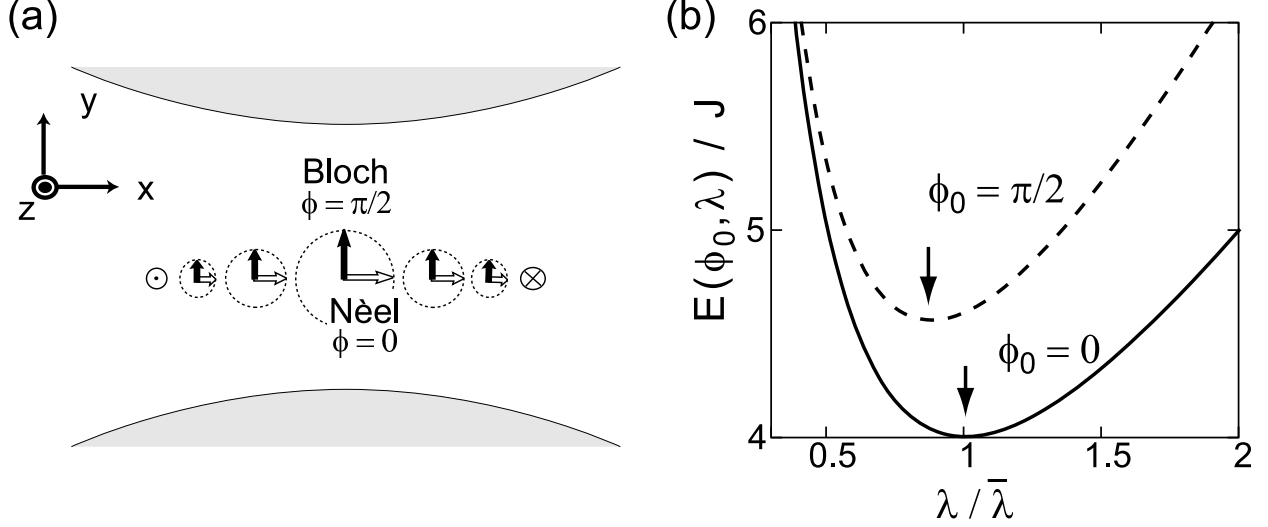


FIG. 1: (a) Bloch and Neél walls confined in a magnetic wire are schematically shown. The regions outside the wire are represented by shading. The solid and hollow arrows represent the magnetization vector of the Bloch and Neél walls, respectively. The dotted circles represent the uniform rotation where the exchange energy of the domain wall takes a constant value. (b) Potential energies are plotted against the width of the domain wall  $\lambda$  for  $\phi_0 = 0$  (solid line) and  $\phi_0 = \pi/2$  (dashed line). The horizontal axis is normalized by the width of the domain wall of the ground state for  $\phi_0 = 0$ . The energy minima are indicated by arrows.

shape, as shown in Fig. 1(a). For simplicity, we modeled the system as a one-dimensional domain wall along the  $x$ -axis with a confining potential, where the directions of the magnetization vectors are represented as  $\mathbf{M} = (\sin \theta \cos \phi, \sin \theta \sin \phi, \cos \theta)$ , where  $\theta$  and  $\phi$  denote, respectively, polar and azimuthal angles for each position. We assume that the system has a bi-axial anisotropy such that the  $z$ - and  $y$ -axes are easy and hard axes, respectively.

Let us begin with a brief introduction of the theory of a one-dimensional domain wall<sup>19,20,21,22</sup>. In the absence of current and confining potential, the energy of the system is expressed as

$$E = \int_{-\infty}^{\infty} dx J [\theta'^2 + \sin^2 \theta \phi'^2] + K_e \sin^2 \theta [1 + r \sin^2 \phi], \quad (1)$$

where the primes denote differentiation with respect to spatial  $x$  coordinate. The first term is the exchange stiffness energy with a stiffness constant of  $J$ . The second term represents the bi-axial anisotropy characterized by the anisotropy constant for the easy axis,  $K_e$ , and the ratio,  $r = K_h/K_e$ , where  $K_h$  is the anisotropy constant for the hard axis.

It should be noted that if the system has uni-axial anisotropy, i. e.,  $r = 0$ , the ground state is degenerate with respect to the azimuthal angle  $\phi$  which is independent of the spatial coordinate. Since the magnetization vectors of the top and bottom electrodes are aligned parallel to the  $z$ -axis, the Bloch and Néel walls correspond to the azimuthal angle of  $\phi = \pi/2$  and  $\phi = 0$ , respectively. The magnetization vectors of the other ground states lie on the dotted circles as shown in Fig. 1(a). The polar angle configuration  $\theta$  of the ground state is given by

$$\theta(x) = \arccos \left[ \tanh \left( \frac{x}{\lambda} \right) \right], \quad (2)$$

where  $\lambda = \sqrt{J/K_e}$  is the domain wall thickness. The degeneracy of the ground state with respect to the azimuthal angle  $\phi$  is broken if the system has bi-axial anisotropy, i.e.,  $r \neq 0$ . Assuming that the azimuthal angle  $\phi$  is independent of the spatial coordinate, the polar angle configuration of the minimum energy state for each value of  $\phi$  is expressed by Eq. (2) with  $\lambda = \bar{\lambda} (1 + r \sin^2 \phi)^{-1/2}$ , where  $\bar{\lambda} = \sqrt{J/K_e}$  represents the domain wall thickness of the ground state with  $\phi = 0$ .

Since we are not interested in the domain wall propagation along the wire but in the breathing-mode excitation, we assume that the domain wall is confined in a certain region of the wire by a confining potential  $V_{cf}$ . We also assume that the characteristic length of  $V_{cf}$  is much larger than  $\bar{\lambda}$ . We adopt  $\phi_0$ ,  $X$  and  $\lambda$  as collective coordinates<sup>23,24</sup>. Here  $\phi_0$  is defined by

$$\phi_0 = \frac{1}{2\lambda} \int_{-\infty}^{\infty} dx \phi \sin^2 \theta, \quad (3)$$

and  $X$  is defined through the polar angle configuration of the ground state,  $\theta_0$ , given by

$$\theta_0 = \arccos \left[ \tanh \left( \frac{x - X}{\lambda} \right) \right], \quad (4)$$

where  $X$  denotes the position of the domain wall center. Substituting Eqs. (3) and (4) into Eq. (1) as  $\theta = \theta_0 + (\theta - \theta_0)$  and  $\phi = \phi_0 + (\phi - \phi_0)$ , and ignoring the spin-wave excitation of  $\theta - \theta_0$  and  $\phi - \phi_0$ , the energy of the domain wall is obtained as

$$E(\phi_0, \lambda) = \frac{2J}{\lambda} \left[ \frac{\bar{\lambda}}{\lambda} + \frac{\lambda}{\bar{\lambda}} (1 + r \sin^2 \phi_0) \right]. \quad (5)$$

In Fig. 1(b) we plot the domain wall energy of Eq. (5) with  $r = 0.3$  as a function of the normalized domain wall thickness  $\lambda/\bar{\lambda}$ . The solid and dotted lines correspond to  $\phi_0 = 0$  and  $\pi/2$ , respectively. As shown in Fig. 1(b), the value of  $\lambda$  which minimizes the domain wall

energy depends on  $\phi_0$ . Therefore, if the precession of the domain wall around the azimuthal axis is induced by an applied current, the oscillation of  $\lambda$  and therefore the resistance of the domain wall are also induced.

For simplicity we assume that the confining potential takes the form  $V_{\text{cf}} = F_0 L [\sinh^2(X/L)]$ , where  $F_0$  and  $L$  represent the magnitude and the characteristic length of the confining potential. As mentioned above we also assume that the characteristic length  $L$  of the confining potential is much longer than the thickness of the domain wall  $\lambda$ . Thus the domain wall thickness is not related to  $L$  and the domain wall is different from the so-called geometrically confined domain wall whose thickness is determined by  $L^{25}$ .

In order to systematically derive the equation of motion described by the collective coordinates, we adopt the Lagrangian method<sup>21,22,26,27</sup>. The Lagrangian corresponding to the torque exerted on magnetizations of the domain wall by an applied current<sup>26,27</sup> is given by

$$- \int_{-\infty}^{\infty} dx \frac{\mu_B P j_e}{(1 + \xi^2) \gamma e} \phi' [1 - \cos \theta], \quad (6)$$

where  $\xi$  is the ratio between the precession time due to the exchange interaction and the spin relaxation time for spin accumulation;  $e$  is the electric charge of an electron;  $j_e$ , the charge current density;  $P$ , the spin polarization of the charge current and  $\gamma$ , the gyromagnetic constant. Then the total Lagrangian of the system under the applied current<sup>21,22,27</sup> is given by

$$\begin{aligned} \mathcal{L} = & \frac{1}{\gamma} \int_{-\infty}^{\infty} dx (\dot{\phi} - j \phi') [1 - \cos \theta] \\ & - J \int_{-\infty}^{\infty} dx [\theta'^2 + \sin^2 \theta \phi'^2] \\ & - K_e \int_{-\infty}^{\infty} dx \sin^2 \theta [1 + r \sin^2 \phi] - V_{\text{cf}}, \end{aligned} \quad (7)$$

where  $j = \mu_B P j_e / (1 + \xi^2) e$  represents the spin-current density. The dots denote differentiation with respect to time  $t$ . In order to obtain the effective Lagrangian described by the collective coordinates  $X$ ,  $\phi_0$  and  $\lambda$ , we substitute  $\theta_0$  and  $\phi_0$  for  $\theta$  and  $\phi$  in Eq. (7), respectively, and then perform integration with respect to  $x$ . We obtain the following effective Lagrangian,

$$\mathcal{L} = \frac{2}{\gamma} (\dot{X} + j) \phi_0 - \frac{2J}{\lambda} - 2\lambda K_d (1 + r \sin^2 \phi_0) - V_{\text{cf}}. \quad (8)$$

In the Lagrangian formalism, the effect of the Gilbert damping<sup>29</sup> is conventionally taken into account by the Rayleigh dissipative function method<sup>22,30</sup>. The dissipation function is

defined by

$$\mathcal{F} = \frac{\alpha}{2\gamma} \int dx \left\{ \left( \dot{\theta} - \frac{\beta}{\alpha} j \theta' \right)^2 + \sin^2 \theta \left( \dot{\phi} - \frac{\beta}{\alpha} j \phi' \right)^2 \right\}, \quad (9)$$

where  $\alpha$  is the Gilbert damping constant. The terms proportional to  $\beta$  reproduces so-called  $\beta$ -term<sup>26,31,32,33,34</sup> and describes drift effect<sup>35</sup>. One can easily confirm that Eq. (9) reproduces the torques coming from the Gilbert damping and  $\beta$  terms as  $-\mathbf{M} \times \delta \mathcal{F} / \delta \dot{\mathbf{M}} = -\alpha \mathbf{M} \times \dot{\mathbf{M}} + \beta j \mathbf{M} \times \mathbf{M}'$ . In order to obtain the effective dissipation function described by the collective coordinates  $X$ ,  $\phi_0$  and  $\lambda$ , in the same way as the derivation of the effective Lagrangian, we substitute  $\theta_0$  and  $\phi_0$  for  $\theta$  and  $\phi$ , respectively, and then perform integration for the coordinate  $x$ . We obtain the following effective dissipation function,

$$\mathcal{F} = \frac{\alpha}{\gamma} \left\{ \frac{\dot{X}^2}{\lambda} + \lambda \dot{\phi}_0^2 + \frac{\pi^2}{12} \frac{\dot{\lambda}^2}{\lambda} + \frac{2\beta}{\alpha\lambda} j \dot{X} \right\}, \quad (10)$$

where the terms which is independent of the time derivatives of the collective coordinates are dropped.

The equation of motion for the domain wall is obtained by using the effective Lagrangian of Eq. (8), the effective dissipation function of Eq. (10) and the Euler-Lagrange equation,

$$\frac{\partial}{\partial t} \frac{\delta \mathcal{L}}{\delta \dot{q}} = \frac{\delta \mathcal{L}}{\delta q} - \frac{\delta \mathcal{F}}{\delta \dot{q}}, \quad (11)$$

where  $q$  being in  $X$ ,  $\phi_0$  and  $\lambda$ . After some algebra we obtain

$$\dot{\phi}_0 + \alpha \frac{\dot{X}}{\lambda} = -\frac{\beta}{\lambda} j + \gamma F_{\text{cf}}^X(X), \quad (12)$$

$$-\dot{X} + \alpha \bar{\lambda} \dot{\phi}_0 \frac{\lambda}{\bar{\lambda}} = j - \gamma \frac{rJ}{\bar{\lambda}^2} \lambda \sin 2\phi_0, \quad (13)$$

$$\frac{\pi^2 \alpha}{12\gamma} \dot{\lambda} = \frac{J}{\bar{\lambda}} \left[ \frac{\bar{\lambda}}{\lambda} - \frac{\lambda}{\bar{\lambda}} \left( 1 + \frac{r}{2} (1 - \cos 2\phi_0) \right) \right], \quad (14)$$

where  $F_{\text{cf}}^X = -\partial_X V_{\text{cf}}$ . Equations (12), (13) and (14) reduces to Slonczewski's equation of domain wall motion<sup>36,37</sup> when the dissipation for dynamics of  $\lambda$  is neglected. The  $\beta$ -proportional term in Eq. (12) represents the torque from the so-called  $\beta$ -term of the Landau-Lifshitz equation<sup>39</sup>. We note that  $\lambda$  is a dynamical variable and is independent of  $\phi_0$  in Eqs. (12)-(14)<sup>38</sup>.

We performed numerical simulations based on Eqs. (12)-(14). The equations were solved using the implicit Runge-Kutta method. Since the confinement force,  $F_{\text{cf}}^X$ , is much larger than the  $\beta$ -term in the present situation, we ignored the first term of the right-hand-side

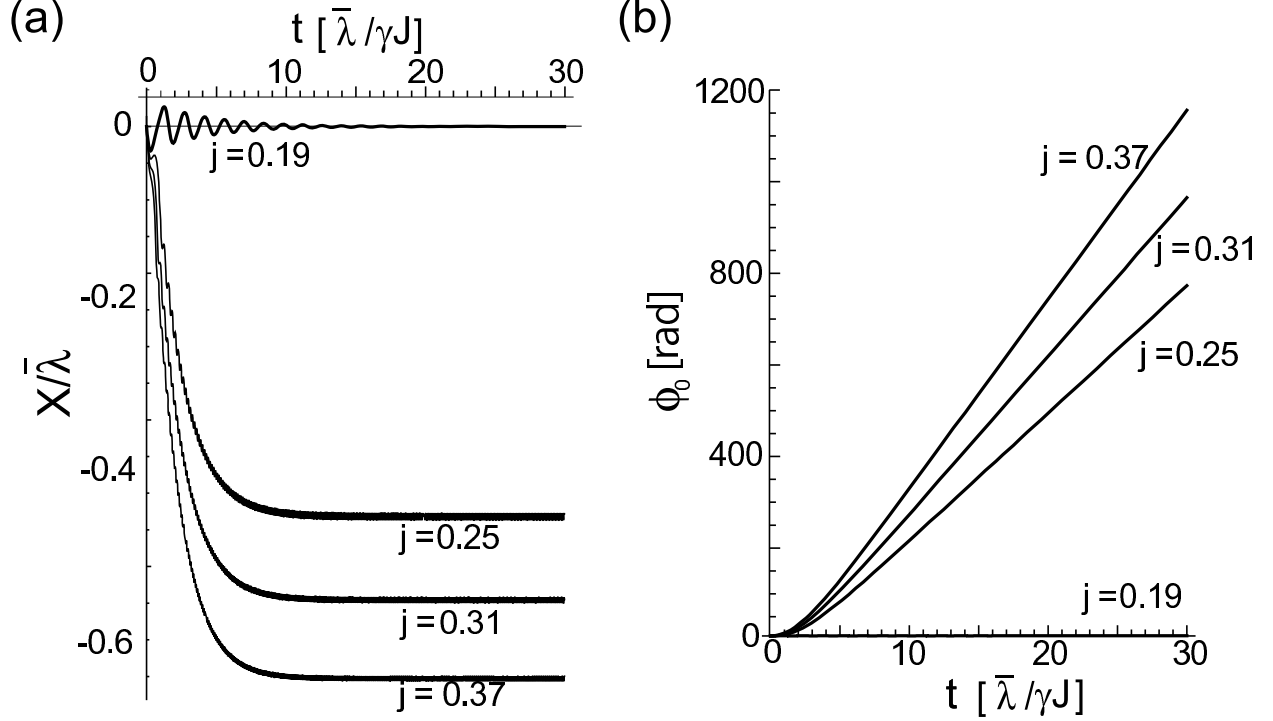


FIG. 2: (a) The position of the domain wall  $X$  is plotted as a function of time  $t$ . The current densities are taken to be  $j = 0.37, 0.31, 0.25$  and  $0.19$  for top to bottom. The unit of the current density is taken to be  $\gamma J/\bar{\lambda}$ . (b) The angle  $\phi_0$  is plotted as a function of time  $t$ . The plot for  $j = 0.19$  lies on the horizontal axis. In both panels, the unit of time is taken to be  $\bar{\lambda}^2/(\gamma J)$ .

of Eq. (12). We took the parameters of the confining potential to be  $L = 2.0\bar{\lambda}$ , and  $F_0 = 100.0J/\bar{\lambda}^2$  to efficiently confine the domain wall to the confinement region. This condition corresponds to the case in which the cross section of the wire exponentially increases tenfold in the linear dimension by the displacement to  $X = L$  from 0. We also set the Gilbert damping constant at 0.01 to reproduce typical experimental systems. At initial time  $t = 0$ , the thickness, position, and azimuthal angle were taken to be  $\lambda = \bar{\lambda}, X = 0$ , and  $\phi_0 = 0$ , respectively.

In Figs. 2(a) and 2(b) we plot the position  $X$  and the angle  $\phi_0$  of the domain wall as a function of time for various values of  $j$ , respectively. The current is switched on at  $t = 0$  and then is kept fixed. As long as the spin-current density  $j$  is smaller than the critical value  $j_c$ , the position of domain wall  $X$  showed little deviation from its initial value of  $X = 0$ . In our simulation  $j_c = 0.22 \gamma J/\bar{\lambda}$ . Hereafter, the unit of the spin-current density is taken to be  $\gamma J/\bar{\lambda}$ . As shown in Fig. 2(b), the angle  $\phi_0$  also shows little deviation from its initial

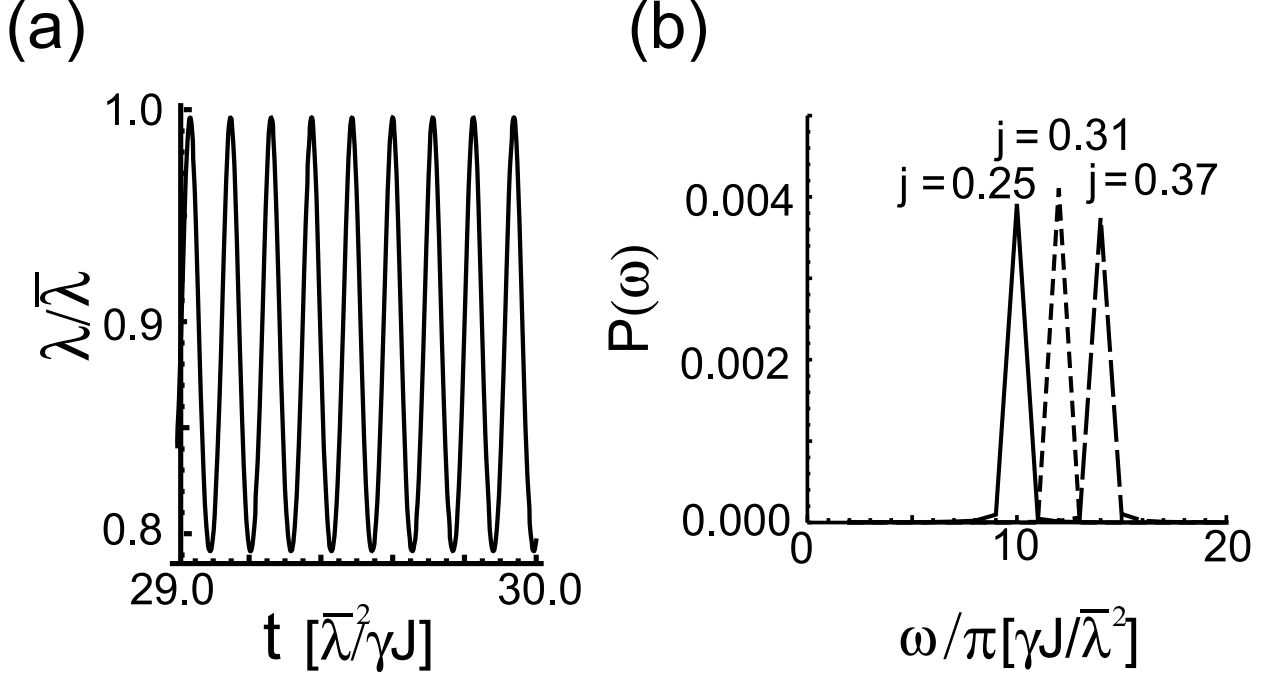


FIG. 3: Thickness oscillation. (a) The normalized width of the domain wall  $\lambda/\bar{\lambda}$  for  $j=0.25$  is plotted as a function of time  $t$ . (b) The power spectrum density  $P(\omega)$  of magnetoresistance obtained by using the theory of Levy and Zhang<sup>16</sup>. Solid, dotted and dot-dashed lines correspond to the current density of 0.25, 0.31, and 0.37, respectively. The unit of the current density is taken to be  $\gamma J/\bar{\lambda}$ .

value  $\phi_0 = 0$  for  $j = 0.19 < j_c$ . Above the critical current,  $j \geq j_c$ ,  $X$  moves to a certain position which is determined by the competition between the confining potential and the spin-transfer torque. The angle  $\phi_0$  linearly increases with increasing time and the domain wall precesses around the  $x$ -axis.

The depinning of the angle  $\phi_0$  shown in Fig. 2(b) is similar to Walker's breakdown<sup>21,37</sup>. However, the  $j_c$  we obtained is not equal to Walker's threshold  $j_W = rJ/\bar{\lambda}$ . As we shall show later, the difference in  $j_c$  and  $j_W$  reflects the essential difference in dynamics between confined and unconfined domain walls, such that coexistence of the oscillation and pinning states for  $j < j_W$  depends on the confining potential.

Since the system has bi-axial anisotropy, the precession of the domain wall induces the oscillation of the domain wall thickness  $\lambda$ , the breathing mode<sup>17</sup>, as shown in Fig. 3(a). According to Levy and Zhang's theory<sup>16</sup>, the resistance  $\Delta R$  of a domain wall depends on its thickness as  $\Delta R \sim 1/\lambda$ . Thus, the resistance  $\Delta R$  oscillates due to the breathing mode.



In Fig. 3(b) we plot the power spectrum density of  $(\bar{\lambda}/\lambda) \sim \Delta R$  defined as

$$P(\omega) = \int d\tau e^{-i\omega\tau} \int dt \frac{\bar{\lambda}^2}{\lambda(t)\lambda(t-\tau)}. \quad (15)$$

For  $j > j_c$ , the oscillation in  $\Delta R$  was observed as expected above. For the typical experimental situation the frequency is on the order of several tens GHz<sup>15</sup>. For each value of  $j$ ,  $P(\omega)$  has a single sharp peak. This means that the system is a useful candidate for a microwave source. The peak frequency of the power spectrum is proportional to  $j$ , which means that we can control the microwave frequency by the current.

The intensity at the peaks is on the order of 0.01 and depends on the amplitude of the thickness oscillation. In this case the amplitude of the thickness oscillation is on the order of  $0.1\bar{\lambda}$ . The value of the intensity is consistent with the amplitude of the thickness oscillation because  $P(\omega)$  is proportional to the square of the amplitude normalized by  $\bar{\lambda}$ . The amplitude of the oscillation is about  $\bar{\lambda}r$ . Thus, the intensity is controlled by the ratio of anisotropy constants,  $r$ , and does not depend on  $j$ . We note that  $\lambda$  is always shorter than  $\bar{\lambda}$  as shown in Fig. 3(a). Namely  $\lambda$  does not agree with the thickness minimizing Eq.(5) because of the effect of the Gilbert damping in Eq. (14)<sup>38</sup>.

Next we move onto adiabatic current sweeping. The current was adiabatically increased from 0 to 0.4 which is above Walker's threshold current  $j_W$ , and then was adiabatically decreased from 0.4 to 0. From Eq. (14), the frequency of the breathing mode in the steady state is related to the velocity of  $\phi_0$  as  $f_0 \equiv \dot{\phi}_0/\pi$ . Figure 4 shows the breathing-mode frequency  $f_0$ . As the current increased from 0, the frequency was kept at zero below the threshold current  $j'_c = j_W \lambda_{\min}/\bar{\lambda}$ , where  $\lambda_{\min} \equiv \min \lambda = \bar{\lambda}\sqrt{1-r}$ . When the current reached  $j = j'_c$  in the simulation, the frequency jumped to a certain value and then linearly increased as the current further increased up to 0.4. As the current decreased from 0.4, the frequency linearly decreases down to a much lower current than  $j'_c$ . That is to say, below the threshold current, the breathing and pinning states coexist. The behavior differs surprisingly from that  $\langle \dot{\phi}_0 \rangle \sim \sqrt{j^2 - j_W^2}$ <sup>21</sup> above the threshold current  $j_W$  in Walker's theory, where a unique state is permitted for each current.

The reason for current-dependence behavior of the breathing motion frequency is that the confining potential enables the breathing and pinning states to coexist. In fact we can see two time-averaged solutions of Eqs. (12) - (14) : the pinning solution is  $\langle \dot{X} \rangle = \langle \dot{\phi}_0 \rangle = 0$ ,  $\langle \phi_0 \rangle \sim \arcsin(j\lambda/\gamma r J)/2$  and the breathing solution is  $\langle \dot{X} \rangle = 0$ ,

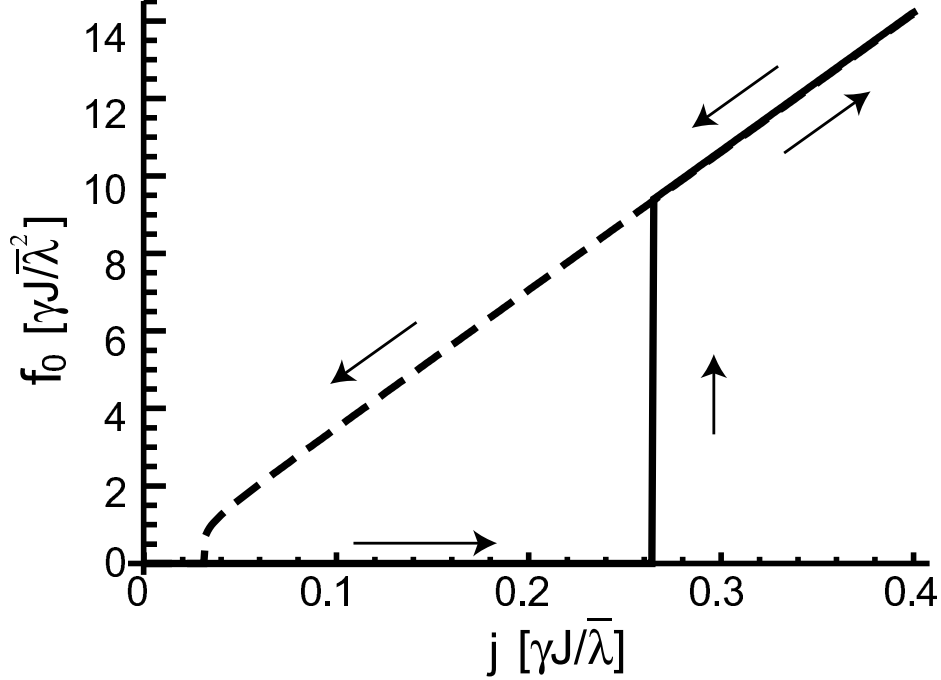


FIG. 4: The breathing-mode frequency  $f_0$  is plotted against the current density  $j$ . A hysteresis loop appears with increasing and decreasing applied current density (indicated by arrows).

$\langle \dot{\phi}_0 \rangle \sim \langle j / \alpha \lambda \rangle \sim \gamma \langle F_{\text{cf}}^X(X) \rangle$ . As mentioned before, the threshold  $j_c$  originates from the coexistence of the two states. We note that if the confining potential does not exist the breathing mode vanishes because  $\langle F_{\text{cf}}^X(X) \rangle = 0$ . The existence of the confining potential induces a drastic effect in the domain wall motion.

In conclusion, we examined the current-induced magnetization dynamics of a domain wall confined in a magnetic wire with bi-axial anisotropy. We showed that breathing-mode excitation, which produces resistance oscillation, is induced by spin-transfer torque. The result means that the confined domain wall is a powerful candidate for a microwave oscillator. We also found that the dependence of the frequency of the breathing mode on the current shows a characteristic hysteresis loop originating from the confining potential.

The authors thank M. Doi, H. Iwasaki, M. Ichimura, K. Miyake, M. Takagishi, M. Sahashi, M. Sasaki, T. Taniguchi, N. Yokoshi and K. Seki for useful discussions. The work was

supported by NEDO and MEXT.Kakenhi(19740243).

---

- <sup>1</sup> J. A. Katine, F. J. Albert, R. A. Buhrman, E. B. Myers, and D. C. Ralph, *Nature* **84**, 4212 (2000).
- <sup>2</sup> M. Tsoi, A. G. M. Jansen, J. Bass, W.-C. Chiang, V. Tsoi, and P. Wyder, *Nature* **406**, 46 (2000).
- <sup>3</sup> S. I. Kiselev, J. C. Sankey, I. N. Krivorotov, N. C. Emley, R. J. Schoelkopf, R. A. Buhrman, and D. C. Ralph, *Nature* **425**, 380 (2003).
- <sup>4</sup> W. H. Rippard, M. R. Pufall, S. Kaka, S. E. Russek, and T. J. Silva, *Phys. Rev. Lett.* **92**, 027201 (2004).
- <sup>5</sup> M. Covington, M. AlHajDarwish, Y. Ding, N. J. Gokemejier, and M. Seigler, *Phys. Rev. B* **69**, 184406 (2004).
- <sup>6</sup> I. N. Krivorotov, N. C. Emley, J. C. Sankey, S. I. Kiselev, D. C. Ralph, and R. A. Buhrman, *Science* **307**, 228 (2005).
- <sup>7</sup> S. Kaka, M. R. Pufall, W. H. Rippard, T. J. Silva, S. E. Russek, and J. A. Katine, *Nature* **437**, 389 (2005).
- <sup>8</sup> F. B. Mancoff, N. D. Rizzo, B. N. Engel, and S. Tehrani, *Nature* **437**, 393 (2005).
- <sup>9</sup> A. N. Slavin and P. Kabos, *IEEE Trans. Magn.* **41**, 1264 (2005).
- <sup>10</sup> S. M. Rezende, F. M. de Aguiar, and A. Azevedo, *Phys. Rev. Lett.* **94**, 037202 (2005).
- <sup>11</sup> J. C. Slonczewski, *J. Magn. Magn. Mater.* **159**, 159 (1996).
- <sup>12</sup> L. Berger, *J. Magn. Magn. Mater.* **54**, 9353 (1996).
- <sup>13</sup> J. C. Slonczewski, *J. Magn. Magn. Mater.* **261**, L26 (1996).
- <sup>14</sup> J. He and S. Zhang, *Appl. Phys. Lett.* **90**, 142508 (2007).
- <sup>15</sup> T. Ono and Y. Nakatani, *Appl. Phys. Exp.* **1**, 061301 (2008).
- <sup>16</sup> P. M. Levy and S. Zhang, *Phys. Rev. Lett.* **79**, 5110 (1997).
- <sup>17</sup> A. L. Dantas, M. S. Vasconcelos, and A. S. Carriço, **226-230**, 1604 (2001).
- <sup>18</sup> A. Thiaville, Y. Nakatani, J. Miltat, and N. Venier, *J. App. Phys.* **95**, 7049 (2005).
- <sup>19</sup> D. Bouzidi and H. Suhl, *Phys. Rev. Lett.* **65**, 2587 (1990).
- <sup>20</sup> H.-B. Braun and D. Loss, *Phys. Rev. B* **53**, 3237 (1996).
- <sup>21</sup> G. Tatara and H. Kohno, *Phys. Rev. Lett.* **92**, 086601 (2004).

- <sup>22</sup> A. Thiaville, J. M. Garcia, and J. Miltat, J. Magn. Magn. Mater **242-245**, 1061 (2002).
- <sup>23</sup> R. Rajaraman, *Solitons and Instantons* (North-Holland, 1982).
- <sup>24</sup> S. Takagi and G. Tatara, Phys. Rev. B **54**, 9920 (1996).
- <sup>25</sup> P. Bruno, Phys. Rev. Lett. **83**, 2425 (1999).
- <sup>26</sup> S. Zhang and Z. Li, Phys. Rev. Lett. **93**, 127204 (2004).
- <sup>27</sup> J. Shibata, G. Tatara, and H. Kohno, **94**, 076601 (2005).
- <sup>39</sup> L. D. Landau and E. M. Lifshitz, Phys. Z. Sowietunion **8**, 153 (1935).
- <sup>29</sup> T. L. Gilbert, Phys. Rev. **100**, 1243 (1955).
- <sup>30</sup> L. D. Landau and E. M. Lifshitz, *Mechanics* (Butterworth-Heinemann, 1982), chap. 25.
- <sup>31</sup> S. E. Barnes and S. Maekawa, Phys. Rev. Lett. **95**, 107204 (2005).
- <sup>32</sup> A. Thiaville, Y. Nakatani, J. Miltat, and Y. Suzuki, Europhys. Lett. **69**, 990 (2005).
- <sup>33</sup> H. Kohno, G. Tatara, and J. Shibata, J. Phys. Soc. Jpn. **75**, 113706 (2006).
- <sup>34</sup> G. Tatara, T. Takayama, H. Kohno, J. Shibata, Y. Nakatani, and H. Fukuyama, J. Phys. Soc. Jpn. **75**, 064708 (2006).
- <sup>35</sup> K. Seki and H. Imamura, Phys. Rev. B **78**, 060402(R) (2008).
- <sup>36</sup> J. C. Slonczewski, Int. J. Magn. **2**, 85 (1972).
- <sup>37</sup> A. Hubert and R. Schäfer, *Magnetic Domains* (Springer-Verlag, 1998).
- <sup>38</sup> One may consider that the oscillation of the domain wall thickness we obtained can be derived by minimizing Eq. (5) in quasistatic limit,  $\lambda = \bar{\lambda} (1 + r \sin^2 \phi)^{-1/2}$ , even without solving Eq. (14). However, as shown in Fig.3(a),  $\lambda$  is not equal to  $\bar{\lambda} (1 + r \sin^2 \phi)^{-1/2}$  in general. The difference between the oscillation of the domain wall thickness obtained by solving Eq. (14) and that of  $\lambda = \bar{\lambda} (1 + r \sin^2 \phi)^{-1/2}$  is essential for the system under high current density. For example, let us consider the case where the time scale of the damping of  $\lambda$  is larger than that of the collective precession of  $\phi_0$ . Such a situation is realized by the large spin-transfer torque under high current density. In such a case  $\lambda$  cannot relax to  $\bar{\lambda} (1 + r \sin^2 \phi)^{-1/2}$  and we have to solve Eq. (14) without quasistatic approximation.
- <sup>39</sup> L. D. Landau and E. M. Lifshitz, Phys. Z. Sowietunion **8**, 153 (1935).